

ESTIMATING NITROGEN CONCENTRATION FROM DIRECTIONAL CHRIS/PROBA DATA

S. Huber^{a, *}, M. Kneubühler^a, B. Koetz^a, J.T. Schopfer^a, N. E. Zimmermann^b and K. I. Itten^a

^a RSL, Dept. of Geography, University of Zurich, Winterthurerstrasse 190, 8057 Zurich, Switzerland - (shuber, kneub, bkoetz, jschopf, itten)@geo.unizh.ch

^b Swiss Federal Research Institute WSL, Land Use Dynamics, Zürcherstrasse 111, 8903 Birmensdorf, Switzerland – niklaus.zimmermann@wsl.ch

KEY WORDS: Biochemistry Retrieval, Subset Selection Algorithm, Multiangular, Continuum Removal, Mixed Forest

ABSTRACT:

Sun and sensor geometry cause directional effects in remotely sensed reflectance data which can influence the estimation of biophysical and biochemical variables. Previous studies have indicated that bidirectional measurements contain added information with which the accuracy of derived plant structural parameters can be increased. Because accurate biochemistry mapping is linked to vegetation structure, nitrogen concentration (C_N) estimates might be indirectly improved with multiangular information. We analyzed data of the spaceborne ESA-mission CHRIS on-board PROBA-1, which provides hyperspectral and multiangular data. The images were acquired in July 2006 over a forest study site in Switzerland and were subsequently preprocessed. From each of the five CHRIS images (five different viewing zenith angles) we extracted 60 crown spectra, which correspond to field-sampled trees. Then we developed four-term models by regressing lab-measured C_N on four datasets either consisting of original reflectance values (SPEC) or continuum-removed data. The wavebands used in the regression models were determined with a subset selection algorithm. For the data of all view angle combinations particular models were generated, in total 31 equations were evaluated per spectral dataset by comparing the coefficients of determination (R^2) and cross-validated root mean square errors. The results of this study indicate that added information contained in multiangular data improved regression models for C_N estimation and lowered RMS errors. Considerable contribution can be achieved with data of a second and third viewing zenith angle. Models based on combinations of off-nadir data performed best. These findings support the potential of multiangular Earth observations for ecological monitoring and modeling studies.

1. INTRODUCTION

Sun and sensor geometry cause directional effects in remotely sensed reflectance data which can influence the estimation of biophysical and biochemical variables. The anisotropic reflectance behavior for instance of plant canopies implies that remotely sensed data can vary without a change in the physical or chemical properties of the material observed. This makes it difficult to interpret remotely sensed data of the same geographic location collected with different instruments, spatial scales or times (Asner, 2004). The bidirectional variability is often considered as noise and its impact on the estimation of plant biochemical and structural variables remains unknown in many cases. However, numerous studies have shown that bidirectional measurements contain added information about vegetation structure (Asner et al., 1998; Barnsley et al., 1997; Meyer et al., 1995), such as leaf area index (Diner et al., 1999), gap fraction and leaf orientation (Chen et al., 2003; Ustin et al., 2004).

The complex vertical and horizontal structure of vegetation communities limits the ability to accurately derive biochemical estimates from remotely sensed data without accounting for canopy structure (Ustin et al., 2004). It has been shown that leaf area index (LAI) and leaf orientation have a strong effect on the expression of leaf optical properties, and thus the biochemistry of foliar material, at canopy scales (Asner, 1998). For canopies with small LAI foliar biochemistry is generally underrepresented. In particular the NIR region, which exhibits the strongest multiple-scattering in green foliage canopies has

the best potential for enhancement of the leaf-level signal (Asner, 1998). So far, there has been little discussion about using directional information to assess biochemical properties such as nitrogen concentration.

The objective of this study was to investigate the influence of anisotropic reflectance effects on the estimation of C_N by evaluating regression models generated on various combinations of CHRIS view angles. We investigated a) if the added information in remotely sensed multiangular data can improve C_N estimates, b) if this information is still present after continuum removal and normalization have been applied to reflectance values and c) if certain sensor view angles or combinations thereof emerge to be beneficial for estimating C_N .

2. DATA AND METHODS

2.1 Study Site

The study site is a mixed forest located in the Swiss Plateau (7°53' E, 47°16' N) at an altitude of about 400–600 meters above sea level. The forest canopy is composed of a mixture of needle-leaf and broadleaf species, dominated by European beech (*Fagus sylvatica* L.), European ash (*Fraxinus excelsior* L.), black alder (*Alnus glutinosa*), silver fir (*Abies alba*) and Norway spruce (*Picea abies* L.). In total nine different species were sampled belonging to two plant functional groups (needle-leaf (evergreen) and broadleaf (deciduous) species).

* Corresponding author.

At the study site we determined 15 subplots where field sampling took place. We selected the subplots according to their species composition to allow the collection of a broad variety of species. At each subplot 3–10 tree crowns were chosen for foliar sampling. The trees selected for leaf collection were chosen regarding crown dimension and species, in order to minimize soil background effects and to gain a broad range of C_N . The species were sampled more or less according to their proportion in the forest.

2.2 Field Data

We collected field data during a two-week field-campaign in July 2004. Foliar material was sampled from the top of tree canopies to determine biochemistry in the laboratory and additional structural and positional tree properties were measured. At the subplots of the study site, a tree climber excised leaf samples of three different upper sunlit canopy branches from a total of 60 trees, whereof 33 were conifers and 27 broadleaves. To obtain representative samples, we collected 15 leaves from all selected deciduous trees and 50–60 needles from the first three needle years from all needle-leaf trees. For each sampled tree the collected leaf material was pooled, sealed in bags and stored in cool environment for transportation. Tree crown dimensions were assessed with a Hypsometer (Haglöf, Sweden). The mean radius of a broadleaf and a needle-leaf tree crown were found to be 5.1 m and 3.2 m, respectively (Huber et al., 2006a). Leaf area index (LAI) was determined with hemispherical photography and ranged from 2.7 to 4.7 m.

In order to geo-locate the sampled tree crowns later in remotely sensed images, the trunk position of each tree was measured during the field campaign with a Trimble GeoXT GPS receiver, which corrects for multipath biases. We improved the positional accuracy by recording 20 to 40 GPS measurements per trunk and applying a post processing differential correction using the Pathfinder Office software (Trimble, 2005). The GPS horizontal precision among all trees ranged from 1.4 to 5.0 m with a mean value of 2.5 m. CHRIS data acquisition took place three years after field data collection but during the same phenological period (July). We assumed a stable C_N level during July (Martin and Aber, 1997) and only small inter-annual variability (Grassi et al., 2005) due to similar climatic conditions in the years of data sampling.

2.3 Laboratory Analyses

In the laboratory, the leaf area, the fresh and dry weight, and the biochemical composition for all 60 collected leaf samples were determined. We used an LI-3100 Area Meter (LI-COR, 1987) to obtain the single-sided leaf area of the samples. Fresh and dry mass were determined by weighing the samples before and after being oven dried at 85° C until a constant weight was achieved. From the difference between the fresh and dry masses divided by the area we calculated water content per cm². For C:N analyses the samples were dried at 65 °C until a constant weight was achieved, then ground to powder and finally injected into an elemental analyzer (NA 2500; CE Instruments, Milan, Italy). Each sample was analyzed twice and checked for within-sample variation. None of the samples exceeded the threshold of 3 % variation of the mean between the two measurements. The measured C_N ranged from 1.00 to 2.97 with a mean of 1.68 and a standard deviation of 0.58 percent by dry weight (Huber et al., 2006b).

2.4 CHRIS Data Acquisition and Processing

In this study we used the data of the spaceborne ESA-mission CHRIS (Compact High Resolution Imaging Spectrometer) on-board PROBA-1 (Barnsley et al., 2004), which provides in mode 5 multiangular data in the range from 447 nm to 1035 nm in 37 bands with a spatial resolution of 18 m. CHRIS supplies five view angles with the nominal fly-by zenith angles (FZA's) at +/-36°, +/-55° and 0° (nadir). The images covered an area of 6.5x13 km and were acquired in July 2006 over the study site Vordemwald.

The FZA's of CHRIS data acquisitions do rarely represent the actual viewing geometry for the date under investigation. The actual view angle for the nadir image was for instance -7.3° in the backward scattering viewing direction (Figure 1).

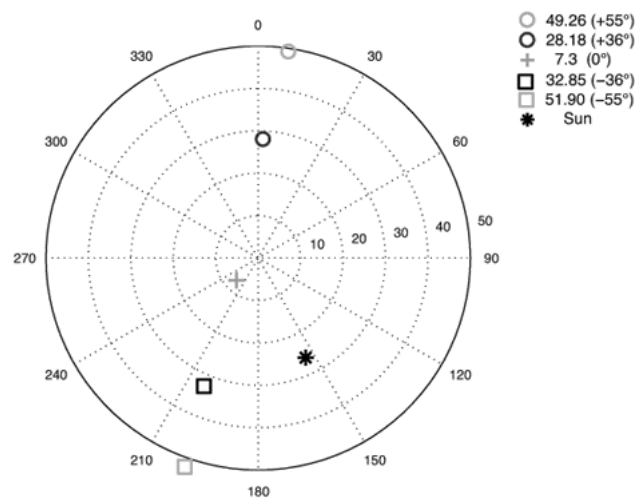


Figure 1. Acquisition geometries and illumination angles for the five CHRIS images acquired on July 1, 2006. The nominal fly-by zenith angles are listed in brackets.

The five CHRIS images were orthorectified and radiometrically corrected (Huber et al., 2006a). Geometric correction was based on a 3D physical model (Toutin, 2004), which is implemented in the commercially available image processing software PCI/OrthoEngine (PCI Geomatics, 2006). High positional accuracy of the respective multiangular products after geometric correction was a prerequisite for a reliable extraction of spectral information from the five images. To achieve a high geometric accuracy, georegistration based on a digital surface model (DSM) (Schläpfer et al., 2003). The resulting RMS errors derived from GCP's were at 0.46–0.79 pixel along track and 0.39–0.73 pixel across track. Subsequent atmospheric correction of the CHRIS radiance data was performed using ATCOR-3 (Richter, 1998), which is based on MODTRAN-4. ATCOR-3 enables the processing of data from tilted sensors by accounting for varying path lengths through the atmosphere, varying transmittance and for terrain effects by incorporating digital terrain models (DTM) data and their derivatives such as slope and aspect, sky view factor and cast shadow. For the atmospheric processing a laser-based DTM with 2 m spatial resolution was resampled to 18 m using bilinear interpolation (Schläpfer et al., 2007).

2.5 Tree Crowns Spectra Extraction and Processing

After geometric and atmospheric correction, tree spectra of the 60 field-sampled crowns were extracted from each of the five CHRIS images. We used the geographical trunk positions (vector data) of the sampled trees to locate the crown pixels in the images (Gorodetzky, 2005) and extracted spectral data with the Region of Interest (ROI) Tool in the ENVI image processing package (Research Systems, 2004). Figure 2 illustrates the different spectral signatures of a Norway spruce obtained from five CHRIS view angles.

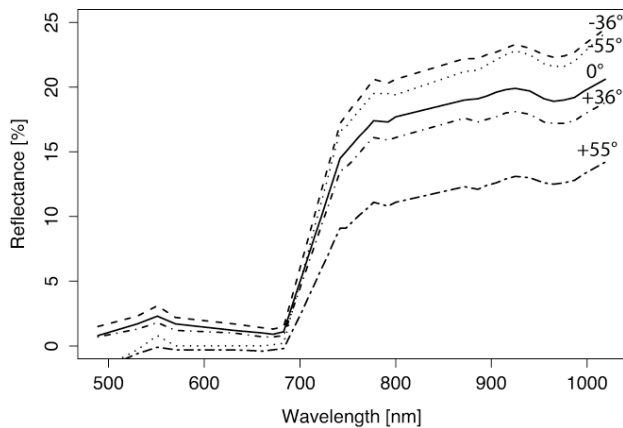


Figure 2. Spectral signatures of Norway spruce from processed CHRIS data of the nominal viewing zenith angles at $-/+36^\circ$, $-/+55^\circ$ and 0° . Negative viewing zenith angles correspond to backward scattering, positive viewing zenith angles represent forward scattering.

For further analyses, four datasets were generated. They either consisted of original reflectance or of continuum-removed data of the five FZA's. The datasets were termed as follows: SPEC included original reflectance values; BNC included band depths normalized to the waveband at the center of the absorption feature, as proposed by Kokaly and Clark (1999); CRDR included continuum-removed derivative reflectance and NBDI included normalized band depth index values, as proposed by Mutanga et al. (2004). Table 1 shows the equations used for the calculation of the datasets.

Continuum removal is a normalization technique and was developed to enhance the spectral features of interest and to minimize extraneous factors, such as atmospheric absorptions, anisotropic effects or soil background effects (Kokaly and Clark, 1999). The observed spectral continuum is considered as an estimate of the other absorptions present in the spectrum, not including the one of interest (Clark and Roush, 1984). To approximate the continuum lines, straight-line segments were used that connect local spectra maxima between 550 and 750 nm. The continuum-removed reflectance (R') is the ratio of the original reflectance values (R) and the corresponding values of the continuum line (R_c) (Kokaly and Clark, 1999). From the continuum-removed reflectance, the band depth (BD) of each point in the absorption feature was computed by subtracting the continuum-removed reflectance (R') from 1.

We applied continuum removal for C_N to the absorption feature located between 550 and 750 nm where the leaf water effect is minimal. Studies have shown a strong nitrogen-pigment relationship because the chlorophyll content in foliage is highly

correlated with total protein and, hence, total nitrogen content (Evans, 1989; Field and Mooney, 1986; Johnson and Billow, 1996; Yoder and Pettigrew-Crosby, 1995). The reason for this is that proteins are the major nitrogen bearing leaf constituents, typically holding 70–80% of all nitrogen. An additional 5–10% of nitrogen is allocated to chlorophyll and lipoproteins (Chapin and Kedrowski, 1983).

Dataset	Equation	Reference
SPEC	R	-
BNC	BD/D_c	(Kokaly and Clark, 1999)
CRDR	$(R'_{(j+1)} - R'_{(j)}) / \Delta_\lambda$	(Mutanga et al., 2004; Tsai and Philpot, 1998)
NBDI	$BD - D_c / BD + D_c$	(Mutanga et al., 2004)

where D_c is the maximum band depth, $R'_{(j)}$ is the continuum-removed reflectance at waveband j , $R'_{(j+1)}$ is the continuum-removed reflectance at waveband $j + 1$, and Δ_λ is the difference in wavelengths between j and $j + 1$.

Table 1. Equations used for the calculations of spectral datasets and corresponding references.

2.6 Statistical Analyses

Multiple linear regression analysis was applied to fit models between C_N (dependent variable) and all possible view angle combinations of the four spectral datasets (SPEC, BNC, CRDR, NBDI). To limit the number of spectral wavebands used in the regression models, this study employed a statistical variable selection method, namely an enumerative branch-and-bound (B&B) search procedure (Miller, 2002). Branch-and-bound algorithms are efficient because they avoid exhaustive enumeration by rejecting suboptimal subsets without direct evaluation (Narendra and Fukunaga, 1977). As a result, a number of wavelengths were selected that best explained C_N . We limited the number of selected wavebands to four to avoid overfitting of the models. All models were tested for significance with the F-test at the 5 % significance level.

An objective of this experiment was to determine whether assessing canopy C_N could be improved with additional directional information. Therefore, we started fitting models on data extracted from one view angle (e.g., nadir). Next, we developed models for all possible combinations of two view angles (e.g., nadir & -36°) and continued the analysis with three and four view angles to finally introduce all view angles as independent variables. In total, 31 view angle combinations were evaluated for each dataset. The findings were evaluated by comparing the mean R^2 for each dataset yielded from models with the same number of view angles involved. The contribution of individual angles was evaluated by considering R^2 values for the correlations between C_N and the spectral data for all angular combinations.

In order to assess the predictive capability of the SPEC based models, cross-validated mean RMS (CV-RMSE) and percentage relative errors (% error) were calculated for each model. We used 10-fold cross-validation with random splitting order of the data (Hastie et al., 2001; Huber et al., 2006b).

We implemented all analyses within the R statistical package, a free software environment for statistical computing and graphics

(R Development Core Team, 2005) under the GNU public license.

3. RESULTS

3.1 Contribution of Angular Information

The contribution of angular information to regression models for estimating C_N is apparent from Figure 3. The coefficient of determination (R^2) increased and CV-RMSEs decreased with additional angular information for all four datasets (SPEC, BNC, CRDR, NBDI). Adding the data of a second angle as independent variables to the regression analyses is contributing most to R^2 , thereafter as more directional information is added as smaller becomes the increase of R^2 . For instance R^2 augmented for the dataset SPEC by 15 %, 8 % and 5 % by adding data of a second, third and fourth view angle, respectively.

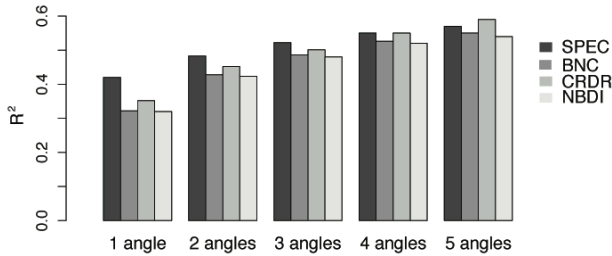


Figure 3. The coefficient of determination (R^2) augmented as more CHRIS view angles were involved in regression analyses. All models consisted of four independent variables.

Evaluating the contribution of directional information by spectral datasets (SPEC, BNC, CRDR, NBDI) revealed interesting differences. Models generated from untransformed reflectance values (SPEC) performed best in terms of R^2 . Only with data of all angles CRDR models performed better ($R^2 = 0.59$).

3.2 View Angle Combinations

R^2 values, CV-RMSEs and percentage relative errors from models developed on data of all possible view angle combinations ($n = 31$) were compared to discover which view angle combinations are promising to improve C_N estimates. This was done for all four datasets. We start reporting the results of monodirectional and continue then with multiangular models.

Best results were achieved with single-angle models based on data of the nominal -36° angle for all datasets except for CRDR, where the -55° angle performed best. Apart from SPEC, models developed on $+36^\circ$ data resulted in the lowest R^2 values (Figure 4). For multi-angle models the combination of off-nadir angles yielded the highest training R^2 values. We obtained maximum R^2 values with data of two viewing zenith angles ($-/+36^\circ$) for BNC (training $R^2 = 0.55$) and NBDI (0.54), whereas SPEC (0.57) and CRDR (0.59) needed data of three viewing zenith angles. The three angles for SPEC were at $-/+36^\circ$ and $+55^\circ$ and for CRDR at $+36^\circ$ and $-/+55^\circ$. Adding data of more than three angles as independent variables to subset selection did not augment the coefficients of variation any further. Thus, the

subset selection algorithm selected the same CHRIS wavebands as for the two or three-angle models.

We used four different reflectance datasets (SPEC, BNC, CRDR and NBDI) to assess whether bidirectional effects are still present after continuum removal. In all continuum-removed datasets R^2 varied considerably for one-angle models. In Figure 4 the variation can be seen for BNC. Additionally, we observed that SPEC performed particularly well for models developed on data of one and two view angles compared to the transformed datasets.

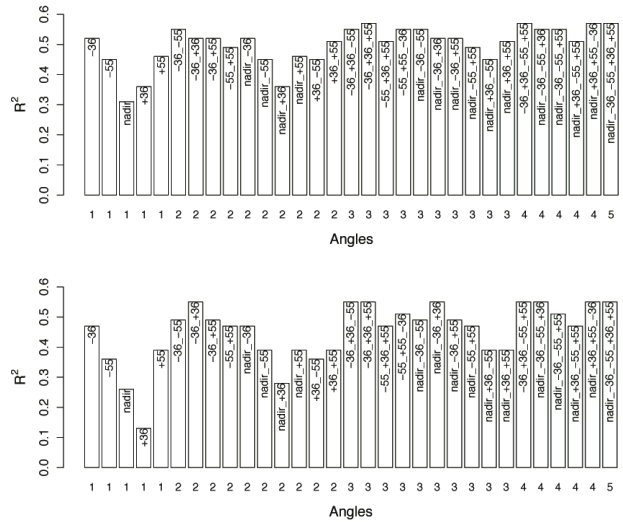
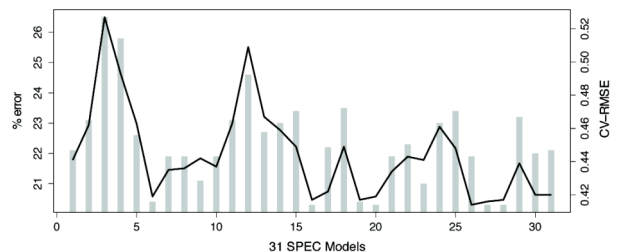


Figure 4. Coefficients of determination R^2 values of C_N regressed on 31 view angle combinations of SPEC (upper) and BNC (lower figure). On the x-axis is the number of view angles provided as independent variables to the regression analyses listed.

Cross-validation revealed that CV-RMSEs and percentage relative errors tend to be smaller with increasing number of view angles involved (Figure 5). For the dataset SPEC, CV-RMSEs ranged from 0.414 to 0.527 % dry weight C_N and relative errors varied between 20.3 and 26.5 %. If we consider both cross-validated measures (CV-RMSE and relative errors) the models based on the angles at -36° and -55° performed best.



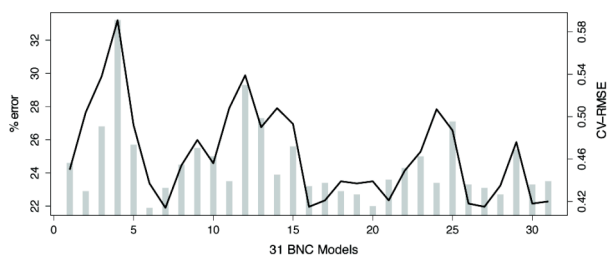


Figure 5. Bars show percentage relative errors (% error) of cross-validated four-term models based on SPEC (upper) and BNC (lower). Root mean square errors (CV-RMSE) are plotted as lines. The x-axis indicates the evaluated 31 models, as higher the number as more view angles were used for regressions.

The CV-RMSE is around 20 % lower compared to the monodirectional nadir model. However, for transformed datasets (BNC, CRDR, NBDI) the combination of backward and forward scattering viewing directions achieved lowest RMSEs. For BNC and NBDI the combination of $-/+36^\circ$ data (CV-RMSE 0.414–0.419) was most promising, for CRDR the combination of $-/+55^\circ$ and $+36^\circ$ data (0.404). We observed larger range of CV-RMSEs for transformed datasets than for SPEC. For all datasets CV-RMSEs of the best model dropped more than 20 % compared to the nadir model.

4. DISCUSSION AND CONCLUSIONS

The study showed that multiangular data improved C_N estimates; R^2 values of regression models increased, for instance from 0.18 (nadir) to 0.57 (three angles) for SPEC, and CV-RMSEs decreased with directional information. In general, CV-RMSEs dropped more than 20 % compared to monodirectional nadir models. This demonstrates that not only the assessment of structural vegetation parameters profit from added information contained in directional reflectance data but also biochemical constituents. These findings support the potential of multiangular Earth observations for ecological monitoring and modeling studies. Further, it points out that biochemistry estimation with wide field of view or sensors with off-nadir viewing capabilities should be interpreted with care.

With four different reflectance datasets (SPEC, BNC, CRDR and NBDI) we assessed whether bidirectional effects are still present after continuum removal. For one-angle models R^2 values varied considerably between view angles for all datasets, indicating that the normalization procedure did not remove all extraneous effects. However, we observed that SPEC performed particularly well for models developed on data of one and two viewing zenith angles. This indicates that untransformed spectral data contains more additional information, for instance about tree structure that possibly improved the regression models. Only starting from four view angles, models developed on continuum-removed datasets improved due to contributing information from additional view angles so that they yielded finally higher R^2 values than SPEC.

In general, monodirectional models trained on data of the -36° viewing zenith angle achieved higher R^2 values than these developed on data of the forward scattering direction. The finding that most information is contained in backward scattering viewing direction reflectance is consistent with other research which found in boreal forests an increase in

bidirectional reflectance in the backward scattering direction but lower reflectance in forward scattering direction, due to a combination of gap and backshadow effects (Deering et al., 1999; Sandmeier et al., 1998). These effects are more pronounced at large source zenith angles and are emphasized in highly absorbing spectral ranges such as the red band due to the lack of multiple scattering in this wavelength range (Deering et al., 1999). It was also shown that the canopy hotspot effect has rich information content for vegetation characterization, especially indications of canopy structure (i.e., a shadow is not visible) (Gerstl, 1999). The viewing zenith angle of -36° is located closest to the images hotspot. The minimum reflectance corresponds to the forward scatter direction because the sensor views the unilluminated, shadowed leaf surfaces (Sandmeier et al., 1998).

For SPEC the model which is solely based on the two angles in the backward scattering direction ($-36^\circ/-55^\circ$) yielded an R^2 (0.55) close to the maximum of 0.57 obtained with at least three view angles and was characterized by low CV-RMSE and % error. On the other hand, two-angle models developed on continuum-removed datasets reached best results by combining reflectance of the forward and backward scattering directions. With three view angles involved no such distinction was observed among datasets. Nadir view direction played a minor role possibly owing to shaded background that is strongest for viewing zenith angles close to nadir (Ni et al., 1999). The large portion of gaps observed in this direction decreases the portion of leaf material seen from the sensor and thus the reflectance values.

This study has investigated the contribution of directional CHRIS data to the estimation of nitrogen concentration by assessing R^2 values and cross-validated RMSEs of regression models fit between the chemical constituent and 31 angular combinations of four spectral datasets. The results of this research show that (1) added information contained in multiangular data improved regression models for C_N estimation and lowered RMS errors ($\sim 20\%$), (2) considerable contribution to R^2 values can be achieved with a second and third viewing zenith angle and (3) models based on combinations of off-nadir data performed best.

ACKNOWLEDGMENT

The authors would like to thank the Swiss National Science Foundation (SNF: project no. 200020-101517) for funding this project. The continuing effort and support of ESA and SIRA to provide CHRIS/PROBA data is gratefully acknowledged. We are very grateful to the Swiss Federal Research WSL and the many individuals who have helped with data collection and processing.

REFERENCES

- Asner, G.P., 2004. Biophysical Remote Sensing Signatures of Arid and Semiarid Ecosystems. In: *Remote sensing for natural resource management and environmental monitoring*. John Wiley & Sons, Hoboken, NJ, pp. 53–109.
- Asner, G.P. et al., 1998. Ecological Research Needs from Multiangle Remote Sensing Data. *Remote Sensing of Environment*, 63(2), pp. 155-165.

- Barnsley, M.J. et al., 1997. On the information content of multiple view angle (MVA) images. *International Journal of Remote Sensing*, 18(9), pp. 1937-1960.
- Barnsley, M.J. et al., 2004. The PROBA/CHRIS mission: a low-cost smallsat for hyperspectral multiangle observations of the Earth surface and atmosphere. *Geoscience and Remote Sensing, IEEE Transactions on*, 42(7), pp. 1512-1520.
- Chapin, F.S. and Kedrowski, R.A., 1983. Seasonal Changes in Nitrogen and Phosphorus Fractions and Autumn Retranslocation in Evergreen and Deciduous Taiga Trees. *Ecology*, 64(2), pp. 376-391.
- Chen, J.M. et al., 2003. Multi-angular optical remote sensing for assessing vegetation structure and carbon absorption. *Remote Sensing of Environment*, 84(4), pp. 516-525.
- Clark, R.N. and Roush, T.L., 1984. Reflectance Spectroscopy: Quantitative Analysis Techniques for Remote Sensing Applications. *Journal of Geophysical Research*, 89(B7), pp. 6329-6340.
- Deering, D.W. et al., 1999. Characterization of the Reflectance Anisotropy of Three Boreal Forest Canopies in Spring-Summer. *Remote Sensing of Environment*, 67(2), pp. 205-229.
- Diner, D.J. et al., 1999. New directions in earth observing: Scientific applications of multiangle remote sensing. *Bulletin of the American Meteorological Society*, 80(11), pp. 2209-2228.
- Evans, J.R., 1989. Photosynthesis and Nitrogen Relationships in Leaves of C₃ Plants. *Oecologia*, 78(1), pp. 9-19.
- Field, C. and Mooney, H.A., 1986. The photosynthesis-nitrogen relationship in wild plants. In: *On the economy of plant form and function: proceedings of the Sixth Maria Moors Cabot Symposium, Evolutionary Constraints on Primary Productivity, Adaptive Patterns of Energy Capture in Plants, Harvard Forest*. Cambridge University Press, Cambridge [Cambridgeshire]; New York.
- Gerstl, S.A.W., 1999. Building a global hotspot ecology with Triana data. In: *Remote Sensing for Earth Science, Ocean, and Sea Ice Applications*. SPIE, Florence, Italy.
- Gorodetzky, D., 2005. Function: `evf_to_rois.sav`, <http://www.itvis.com/codebank/search.asp?FID=93> (assessed 13 Feb. 2007).
- Grassi, G. et al., 2005. Seasonal and interannual variability of photosynthetic capacity in relation to leaf nitrogen in a deciduous forest plantation in northern Italy. *Tree Physiology*, 25(3), pp. 349-360.
- Haglöf (Sweden), <http://www.haglofsweden.com> (accessed 16 Jan. 2007). pp.
- Hastie, T. et al., 2001. *The elements of statistical learning: data mining, inference, and prediction*. Springer, New York, pp. Pages.
- Huber, S. et al., 2006a. Canopy Biochemistry Estimation using Spectrodirectional Information of CHRIS Data. In: *2nd International Symposium on Recent Advances in Quantitative Remote Sensing (RAQRS)*, Torrent (Valencia), Spain.
- Huber, S. et al., 2006b. Estimating Biochemistry in Mixed Forests from HyMap Data using Band-Depth Analyses and Subset Regression Algorithms. In Preparation, pp.
- Johnson, L.F. and Billow, C.R., 1996. Spectrometric estimation of total nitrogen concentration in Douglas-fir foliage. *International Journal of Remote Sensing*, 17(3), pp. 489-500.
- Kokaly, R.F. and Clark, R.N., 1999. Spectroscopic determination of leaf biochemistry using band-depth analysis of absorption features and stepwise multiple linear regression. *Remote Sensing of Environment*, 67(3), pp. 267-287.
- Martin, M.E. and Aber, J.D., 1997. High spectral resolution remote sensing of forest canopy lignin, nitrogen, and ecosystem processes. *Ecological Applications*, 7(2), pp. 431-443.
- Meyer, D. et al., 1995. The effect of surface anisotropy and viewing geometry on the estimation of NDVI from AVHRR. *Remote Sensing Reviews*, 12(1), pp. 3-27.
- Miller, A.J., 2002. *Subset selection in regression*. Chapman & Hall/CRC, Boca Raton, pp. Pages.
- Mutanga, O. et al., 2004. Predicting in situ pasture quality in the Kruger National Park, South Africa, using continuum-removed absorption features. *Remote Sensing of Environment*, 89(3), pp. 393-408.
- Narendra, P.M. and Fukunaga, K., 1977. Branch and Bound Algorithm for Feature Subset Selection. *IEEE Transactions on Computers*, 26(9), pp. 917-922.
- Ni, W. et al., 1999. Variance in Bidirectional Reflectance over Discontinuous Plant Canopies. *Remote Sensing of Environment*, 69(1), pp. 1-15.
- PCI Geomatics, 2006. OrthoEngine, User's Guide Version 10.0.
- R Development Core Team, 2005. R: A language and environment for statistical computing. R Foundation for Statistical Computing., Vienna, Austria.
- Research Systems, 2004. ENVI User's Guide. Research Systems Inc.
- Richter, R., 1998. Correction of satellite images over mountainous terrain. *Applied Optics*, 37, pp. 4004-4015.
- Sandmeier, S. et al., 1998. Physical Mechanisms in Hyperspectral BRDF Data of Grass and Watercress. *Remote Sensing of Environment*, 66(2), pp. 222-233.
- Schläpfer, D. et al., 2003. The influence of DEM characteristics on preprocessing of DAIS/ROSIS data in high altitude alpine terrain. In: *3rd EARSeL Workshop on Imaging Spectroscopy*. EARSeL and DLR, Herrsching, Germany.
- Schläpfer, D. et al., 2007. Spatial PSF Non-Uniformity Effects in Airborne Pushbroom Imaging Spectrometry Data. *IEEE Transactions on Geoscience and Remote Sensing*, accepted., pp. 458-468.
- Toutin, T., 2004. Review article: Geometric processing of remote sensing images: models, algorithms and methods. *International Journal of Remote Sensing*, 25(10), pp. 1893-1924.
- Trimble, 2005. GPS Pathfinder Office Software. Trimble.
- Tsai, F. and Philpot, W., 1998. Derivative Analysis of Hyperspectral Data. *Remote Sensing of Environment*, 66(1), pp. 41-51.
- Ustin, S.L. et al., 2004. Remote Sensing of the Environment: State of the Science and New Directions. In: *Remote sensing for natural resource management and environmental monitoring*. John Wiley & Sons, Hoboken, NJ, pp. 679-729.
- Yoder, B.J. and Pettigrew-Crosby, R.E., 1995. Predicting Nitrogen and Chlorophyll Content and Concentrations from Reflectance Spectra (400-2500nm) at Leaf and Canopy Scales. *Remote Sensing of Environment*, 53, pp. 199-211.